EVOLUTIONARY BIOLOGY

Early tetrapod cranial evolution is characterized by increased complexity, constraint, and an offset from fin-limb evolution

James R. G. Rawson[1]*, Borja Esteve-Altava[2], Laura B. Porro[3], Hugo Dutel[1,4], Emily J. Rayfield[1]*

Copyright © 2022 The Authors, some rights reserved; exclusive licensee American Association for the Advancement of Science. No claim to original U.S. Government Works. Distributed under a Creative Commons Attribution NonCommercial License 4.0 (CC BY-NC).

The developmental underpinnings and functional consequences of modifications to the limbs during the origin of the tetrapod body plan are increasingly well characterized, but less is understood about the evolution of the tetrapod skull. Decrease in skull bone number has been hypothesized to promote morphological and functional diversification in vertebrate clades, but its impact during the initial rise of tetrapods is unknown. Here, we test this by quantifying topological changes to cranial anatomy in fossil and living taxa bracketing the fin-to-limb transition using anatomical network analysis. We find that bone loss across the origin of tetrapods is associated not only with increased complexity of bone-to-bone contacts but also with decreasing topological diversity throughout the late Paleozoic, which may be related to developmental and/or mechanical constraints. We also uncover a 10-Ma offset between fin-limb and cranial morphological evolution, suggesting that different evolutionary drivers affected these features during the origin of tetrapods.

INTRODUCTION

The origin of tetrapods was a transformative event in vertebrate evolution and involved marked changes to the vertebrate body plan, leading to morphological and ecological radiation (*1*, *2*). Our understanding of this transition has advanced in recent years, particularly surrounding the evolution of limbs from fins, through the discovery of previously unknown fossils (*3*–*5*), application of new analytical techniques (*6*, *7*), and understanding of genetics and development (*8*–*11*). Despite a transition from water to land characterizing the origin of tetrapods, many of these postcranial characters are now thought to have evolved in aquatic settings and initially facilitated an aquatic existence (*4*, *12*). The skull also undergoes notable morphological changes across the origin of tetrapods, with a flattening and elongation of the head that is freed from the shoulder girdle via a neck, loss of a flexible intracranial joint, and loss and fusion of skull bones (*2*, *13*, *14*). These seemingly rapid changes have been linked to consolidation and strengthening of the skull to facilitate the shift from aquatic suction feeding in tetrapodomorph fish to terrestrial biting in later tetrapods and from swimming to walking on land (*15*). Recent work has also revealed significantly elevated rates of evolution in the crania of elpistostegalians, including early tetrapods, compared to more basal tetrapodomorphs (*16*). However, both tetrapodomorph fish and early tetrapods likely used a mixture of biting and suction feeding (*14*, *17*–*20*), and morphometric analyses reveal that little morphological or functional change occurred in the lower jaw across the fin-to-limb transition (*12*, *21*). It is unclear whether such features evolved for feeding in water or on land or mixed environments, and the tempo of cranial versus postcranial evolution remains elusive.

The loss and fusion of skull bones is common to a number of evolutionary transitions (*22*–*24*). This apparent mechanism of morphological variation has been correlated with either skull consolidation and muscle reorganization to produce a stronger bite in synapsids (*25*) and turtles (*26*) or increased flexibility of the skull to facilitate cranial kinesis in squamates (*27*) and birds (*28*). This process is referred as to Williston's law, which proposes a trend of multipart structures in organisms tending to reduce the number of elements during evolution but, at the same time, providing a mechanism to increase diversity and functional specialization (*29*). Cranial bones that have fewer contacts are more likely to be lost across tetrapod lineages (*23*), which may influence the evolution of modularity and morphological diversity (disparity). Modifications to bone connections may also reflect functional demands: The presence or absence of cranial bones and the distribution of sutures have important implications for load transfer and the structural resistance of the skull (*30*).

Here, we assess whether similar drivers exist at the origin of the tetrapod skull. We review modifications to cranial anatomy across the origin of tetrapods and in extant bracketing taxa to test whether loss of bones confers simplification or increased topological complexity to the cranium. We also test whether cranial bone count reduction and reorganization acts as a mechanism to promote cranial disparity in early tetrapods or acts as an evolutionary constraint. We then explore how cranial topological disparity evolves across the origin of tetrapods against a backdrop of extinction events and anatomical and functional modifications to the fin-limb and axial skeleton. By using a network analysis approach (*31*), where the cranial bones are modeled as a network with nodes representing bones and links representing sutural connections, we quantify how skull bones are arranged and interrelated, the so-called cranial bone topology. Topological complexity of the skull can be measured based on the properties of the connections between the bones (or nodes): Networks where each node has a greater average number of links to nearby nodes are considered as being more complex. We measured eight topological variables to quantify the organization of these skull networks (data S2); see Fig. 1 for a full explanation of the variables measured and our modeling approach. We tabulated these variables in the cranial anatomy of 76 extinct taxa and 34 extant taxa (Fig. 2) using literature descriptions and available retrodeformed three-dimensional (3D) models

[1]School of Earth Sciences, University of Bristol, Bristol BS8 1RJ, UK. [2]Institut de Biologia Evolutiva, Departament de Ciències Experimentals i la Salud, Universitat Pompeu Fabra, Barcelona, Spain. [3]Centre for Integrative Anatomy, Department of Cell and Developmental Biology, UCL, Gower Street, London WC1E 6BT, UK. [4]Department of Engineering, University of Hull, Cottingham Road, Hull HU6 7RX, UK.
*Corresponding author. Email: jr17384@bristol.ac.uk (J.R.G.R.); e.rayfield@bristol.ac.uk (E.J.R.)

(data S1). Our study was enhanced by the use of new 3D datasets of key taxa across the transition, captured via x-ray computed tomography (CT) scans (*17*, *18*, *32*, *33*).

RESULTS

Topological changes across the fish-tetrapod transition

To quantify and compare the cranial architecture of extant fish (non-tetrapod vertebrates), extant tetrapods, and early tetrapod fossils, we performed a principal component analysis (PCA) to capture the variance across the eight variables describing cranial bone topology (Fig. 3). Our results show that fish and tetrapods have distinct skull bone topologies and occupy significantly different areas of topological space [pairwise permutational multivariate analysis of variance (PERMANOVA), $F_{1,111} = 16.164$, $P = 9.9 \times 10^{-5}$]. An alternative test where the number of bones (N) and the number of links (K) are excluded also supports this difference (PERMANOVA, $F_{1,111} = 13.43$, $P = 9.9 \times 10^{-5}$), indicating that the two groups have distinct cranial bone topology even when bone number is excluded. Furthermore, we found significant anatomical differences between all taxonomic groups (table S1), demonstrating the influence of phylogeny on skull roof morphology.

Fish skulls generally have a high number of bones and connections and are fairly modular. Each bone, on average, is sparsely connected to its neighbors and has a long average path length. By comparison, the skulls of early tetrapods and amniotes have fewer bones, but those that remain are more densely connected, bone topology is less modular, and there are smaller average path lengths between bones. This trend is documented across the first principal axis of variation (48.2% of explained variance), with extant Lissamphibia and the living lungfish *Protopterus* occupying the positive extreme of PC1. The second PC of variation (21.4% of explained variance) discriminates between skulls with bones that have a disparate number of articulations, tend to contact bones with a different number of articulations, and tend to form three-node loops or triads such as caecilians and extinct coelacanths and skulls with bones that have a similar number of connections, preferentially contacting to bones with a similar number of articulations, and that form fewer three-node loops, features that are not exclusive to any group.

The effect of bone loss on skull complexity

To determine whether bone loss confers simplification or increased complexity to skull topology, we carried out a phylogenetic generalized least squares (PGLS) regression to test how each topological variable responded to changes in the number of bones for each taxonomic group (table S2). We find that networks with higher numbers of bones consistently show decreased density across all clades (Fig. 4A), meaning that as skulls lose bones (from fish to early tetrapods and amniotes), they acquire more connections per bone on average and therefore a more complex topology. Extant lissamphibians and *Protopterus*, which have the fewest skull bones, therefore have the most complex skull topology. Parcellation also showed a significant relationship

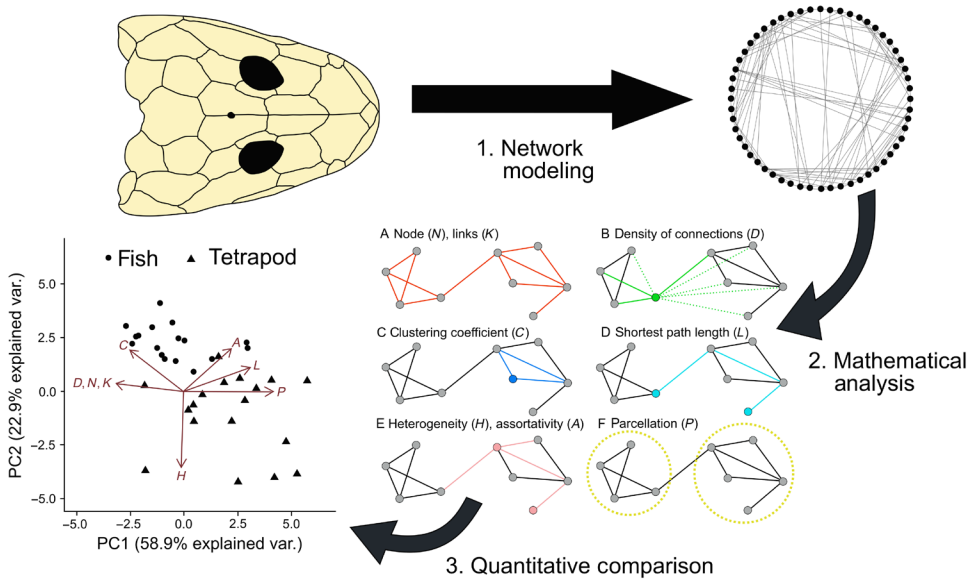

Fig. 1. Pipeline of anatomical network analysis. The skull is coded as an anatomical network and characterized using eight topological variables, shown here on a simplified network (*6*, *23*, *24*). (**A** to **F**) The number of nodes (N) in the network, here colored as gray dots ($N = 9$); the number of links in the network (K), shown as red lines ($K = 12$); density of connections (D) measures the number of connections present divided by the maximum number possible, shown here for just one node. The central node has three realized connections (green solid lines) and five possible but unrealized connections (green dashed lines); mean clustering coefficient (C) measures the likelihood that two connected nodes are also both connected to the same node. The blue node has only two neighbors, which are, in turn, connected to each other (solid blue), forming a three-node loop, C for this node = 1; mean shortest path length (L) is the minimum number of links required to connect two nodes, in this case 3 for the two cyan nodes; heterogeneity (H) measures the anisomerism and irregularity of components in the anatomical structure as the ratio between the SD and the mean of the number of connections of all nodes in the network. Skulls where each bone varies greatly in number of articulations will have a high H; assortativity (A) quantifies the extent to which nodes with the same number of connections connect to each other, whereupon A is more positive; parcellation (P) is the modularity of an anatomical structure and is calculated after a community detection algorithm has identified connectivity modules (yellow dashed circles). Skulls with more network modules and with bones evenly distributed among modules will have a high P. Further mathematical details for calculating topological variables can be found in the Supplementary Materials (Supplementary Text).

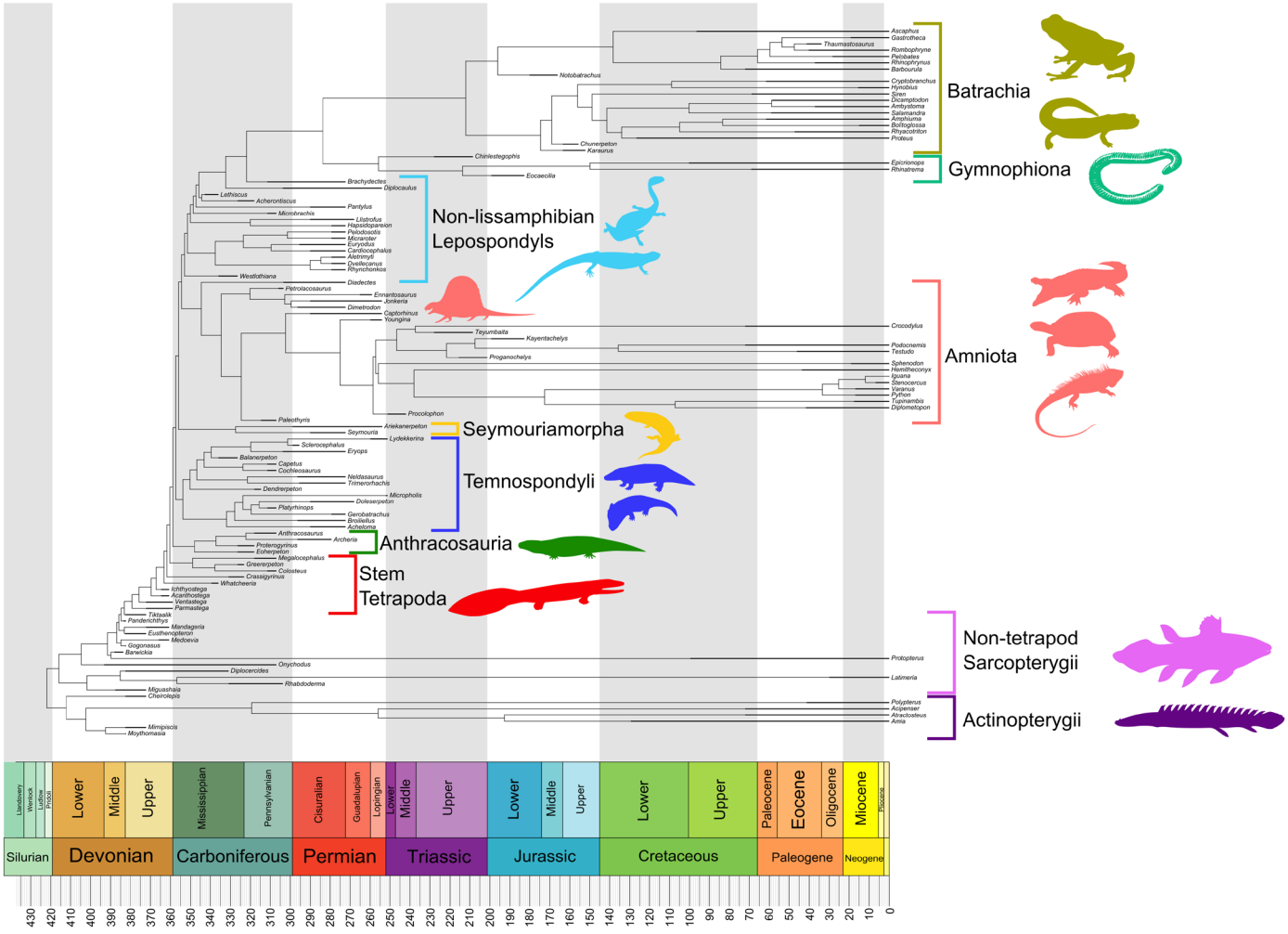

Fig. 2. Time-calibrated phylogeny of vertebrates assembled for this study. Phylogenetic hypothesis of tetrapod relationships shown here is based on the work of Marjanović and Laurin (*52*), wherein lissamphibians are monophyletic within lepospondyls. The alternative topology used in this study based on the work of Ruta *et al.* (*53*) is shown in fig. S1. Example taxon silhouettes were taken from phylopic.org. Credit to Y. Yang (https://creativecommons.org/licenses/by-nc-sa/3.0/), C. C. Julián-Caballero (https://creativecommons.org/licenses/by/3.0/), J. B. McHugh (https://creativecommons.org/licenses/by-nc-sa/3.0/), D. Bogdanov (https://creativecommons.org/licenses/by-sa/3.0/), A. A. Farke and G. Monger (https://creativecommons.org/licenses/by/3.0/), Smokeybjb (https://creativecommons.org/licenses/by-sa/3.0/), N. Tamura (https://creativecommons.org/licenses/by/3.0/), and M. Karala (https://creativecommons.org/licenses/by-nc-sa/3.0/) for taxon silhouettes from Phylopic.

with bone number for early tetrapods, fishes, amniotes, and batrachians (Fig. 4B); skulls with a greater number of bones are split more into distinct modules, whereas those with fewer bones are more integrated into a single unit. This is not the case with caecilians, where reducing bone number does not result in a significantly more integrated skull. Trends for the other topological variables show mixed results in different groups, suggesting that these variables are not strongly affected by reduction in bone number, at least not uniformly across all clades.

Topological disparity through time

We then tested whether evolutionary changes to cranial bone organization led to increased topological disparity over time. Mean relative subclade disparity of our PC scores was used to calculate topological disparity through time (DTT) for two alternate phylogenetic hypotheses. We observe that mean relative subclade disparity in the topology of cranial bones generally decreases from 425 to 250 million years (Ma), with a slight increase in the Late Palaeozoic (Fig. 5A). To test whether the disparity over the entire time range was statistically different from what we might expect from stochastic evolution, we performed a randomization inference test with 10,000 simulations under a Brownian motion model of evolution and compared it to the morphological disparity index (MDI) for our DTT trend line. We found that the DTT profile shows a statistically significant deviation from the 95% confidence interval, regardless of the phylogenetic hypothesis used (tree A: MDI = −0.187, $P = 4.03 \times 10^{-85}$; tree B: MDI = −0.187, $P = 4.03 \times 10^{-85}$). Negative MDI values indicate that the mean relative subclade disparity was lower than expected in both trees, showing that our measurements of topological disparity depict a decrease in disparity over time that cannot be entirely explained by stochastic evolution.

We lastly explored how variation in the topological disparity of the skull relates to extinction events and anatomical modifications to the postcranial skeleton. Topological disparity is low from around

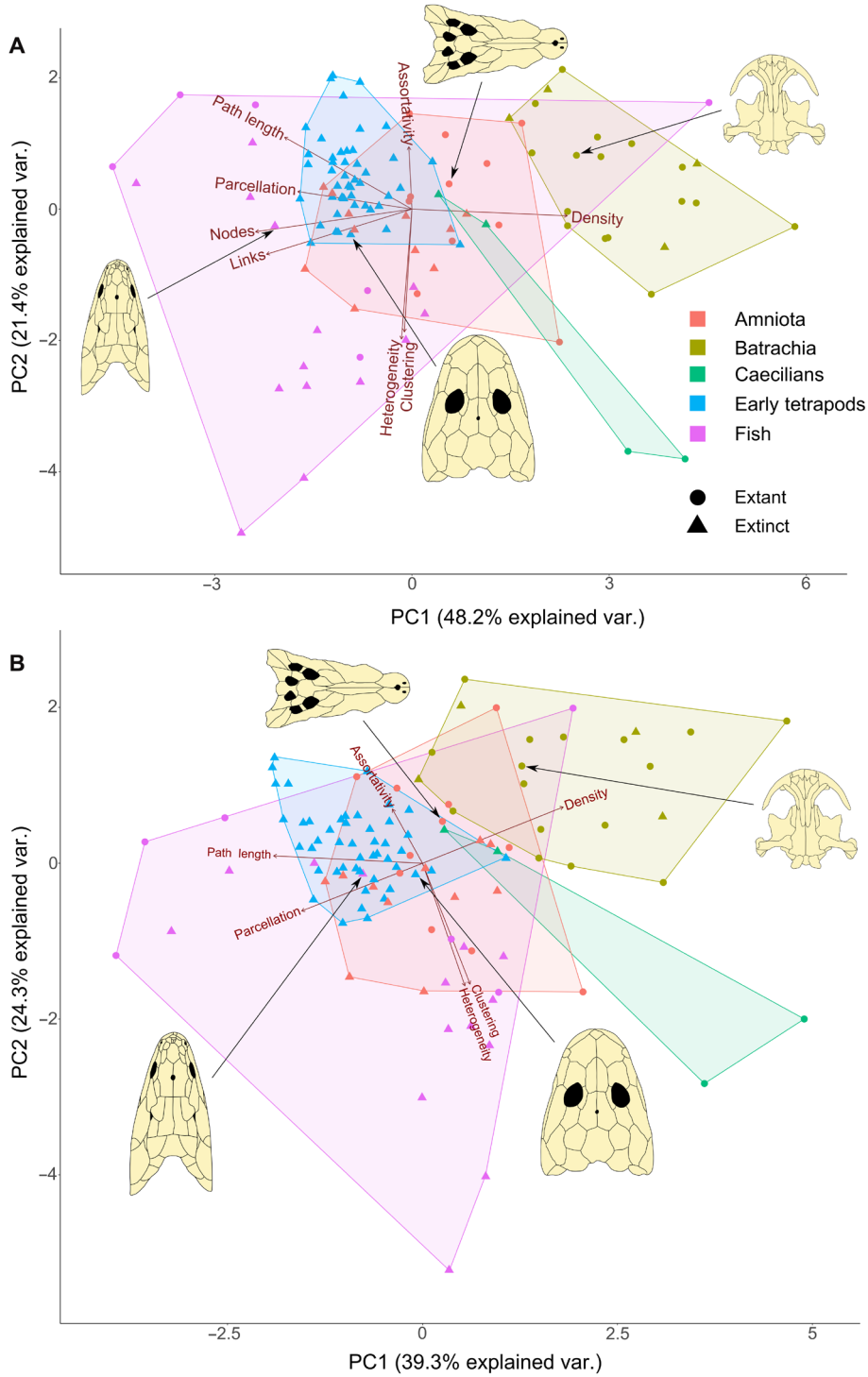

Fig. 3. Discrimination of skull networks by taxonomic group. (**A**) PCA including all eight topological variables. (**B**) PCA excluding the number of nodes (*N*) and number of links (*K*). Red arrows show the relative contribution of each variable to the principal axes. Representative skulls in dorsal view are shown for each group: *Eusthenopteron* (*74*), *Ichthyostega* (*1*), *Cryptobranchus* (*75*), and *Crocodylus* (*76*).

425 Ma, rises sharply, and then declines between the earliest tetrapod footprints (*34*) and osteological evidence for the first tetrapods at 380 Ma (*35*). At this point, cranial topological disparity drops below the 95% confidence intervals, indicating a disparity significantly lower than that expected of Brownian motion for the first time in the tetrapod lineage. Disparity remains constantly low until around 360 Ma when it drops sharply at end of the Devonian, a period also associated with a decrease in taxon sampling in our data (fig. S4). Despite an increase in taxon sampling in the Carboniferous, cranial topological disparity remains low throughout this period and only

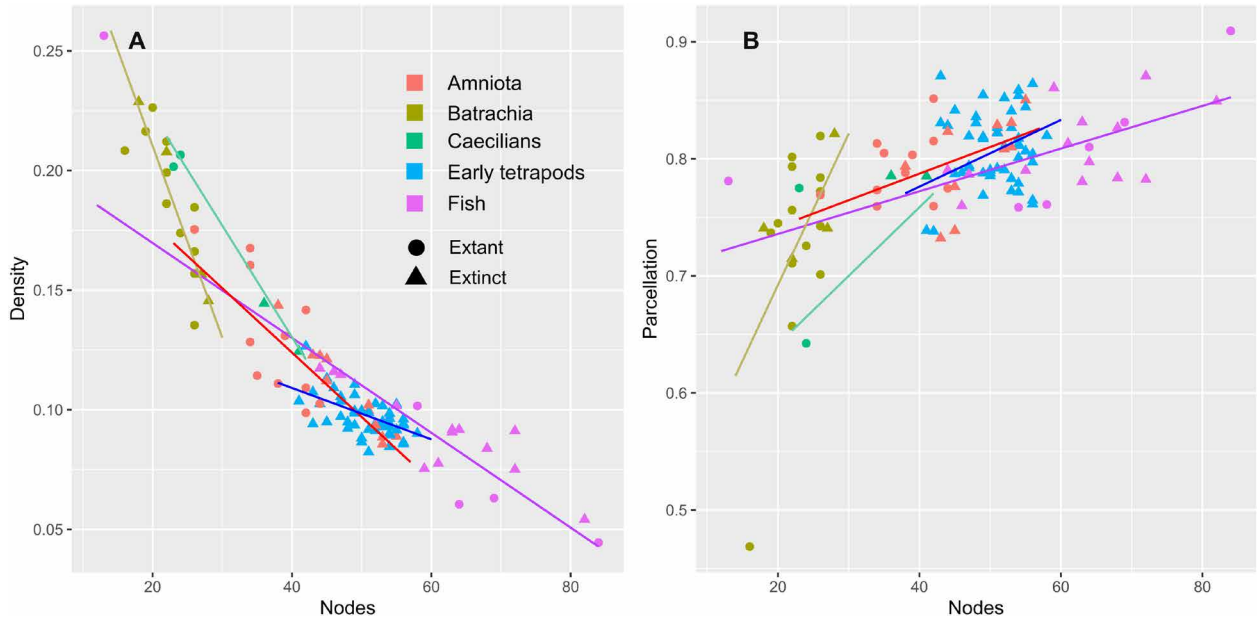

Fig. 4. Response of key topological variables to bone loss. Bone number (*N*) plotted density (**A**) and parcellation (**B**) for each species, split by taxonomic group. Graphs for the remaining topological variables can be found in fig. S2. The best-fitted line calculated by PGLS is shown for each group, calculated using the Marjanović and Laurin (*52*) topology [equivalent figures for the Ruta *et al.* (*53*) topology are found in fig. S3 but are largely unchanged].

begins to increase gradually in the very Late Carboniferous at around 318 Ma before stabilizing throughout much of the Permian. Comparing our data to the DTT profile of pectoral and pelvic appendages across this period (Fig. 5, B and C), previously published by Esteve-Altava *et al.* (*6*), we see that the trend is broadly similar, with an initially higher disparity showing a marked drop below the 95% confidence intervals somewhere close to the midpoint of the Devonian. However, the spike in skull topological disparity during the Middle Devonian is not present in the limbs, and the drop below the 95% confidence interval in limbs precedes the drop seen in the skull by approximately 10 Ma. There is also no marked drop in limb topological disparity at the end of the Devonian, only a continuation of the very slight downward trend. Topological changes to the tetrapod cranium during the Palaeozoic therefore do not occur in parallel to changes in the appendages.

DISCUSSION

Our results show that fish and tetrapods have distinct cranial bone topological organization and that this change in cranial anatomy occurs across the origin of the earliest tetrapods. Topological complexity increases across the fish-tetrapod transition: As cranial bone number decreases, the remaining bones acquire more connections (increased density). In contrast, modularity (parcellation) decreases across the origin of tetrapods; skulls with fewer bones are more integrated and less modular. This does not hold true within caecilians, but this may be an artifact of a small sample size. No such modification to topological complexity was found between the first stem tetrapods and crown tetrapods from later in the Palaeozoic, suggesting that increased terrestrialization in crown taxa such as *Eryops* (*36*) compared to aquatic stem taxa such as *Acanthostega* (*12*) did not result in significant change to skull construction. Some groups like snakes and lissamphibians show more specialized skulls (*37*, *38*) with greatly reduced bone number compared to early tetrapods, but these specializations did not evolve until much later (*39*, *40*). We therefore found no evidence to support the hypothesis that specific changes in the topology of cranial bones—changes in bone number and connections—followed increased terrestrialization in early tetrapods.

Reduction in bone count can be largely attributed to the loss and fusion of nasal, rostral, and tectal bones during the evolution of tetrapods. Tetrapodomorph fish, even those close to the tetrapod total group such as *Eusthenopteron* and *Panderichthys* (*41*), show a classically "fish-like" mosaic arrangement of bones in the anterior snout, most of which are fused or absent from even the earliest tetrapods such as *Ventastega* (*42*). These numerous bones are small and only contact a few of their neighbors, thus decreasing the proportion of realized connections in the networks (thus lower density values in fish). Sparsely connected gill cover bones on the posterior margins of fish skulls also decrease density. Parcellation, the degree of modularity, is increased in the skulls of fish due to a higher degree of separation between distinct modules (e.g., nasoparietal shield, postparietal shield, cheek, and palate), with fewer connections between these modules. Tetrapods show less clear distinction, with the cranium being much more integrated. The topological changes observed across the fish-tetrapod transition supports recent investigations into the mechanisms behind Williston's law, where bones with fewer connections tend to be preferentially lost (*23*, *24*).

Our results do not support the idea that skulls became more densely connected to provide increased support against physical constraint in newly colonized terrestrial environments, since the earliest limbed tetrapods exhibit skulls with reduced bone number (Fig. 3) despite showing evidence for aquatic lifestyles (*5*, *43*). Drastic reduction in skull bone number also occurs across the evolution of lungfish despite their fully aquatic lifestyle (*44*). Function may have driven increased

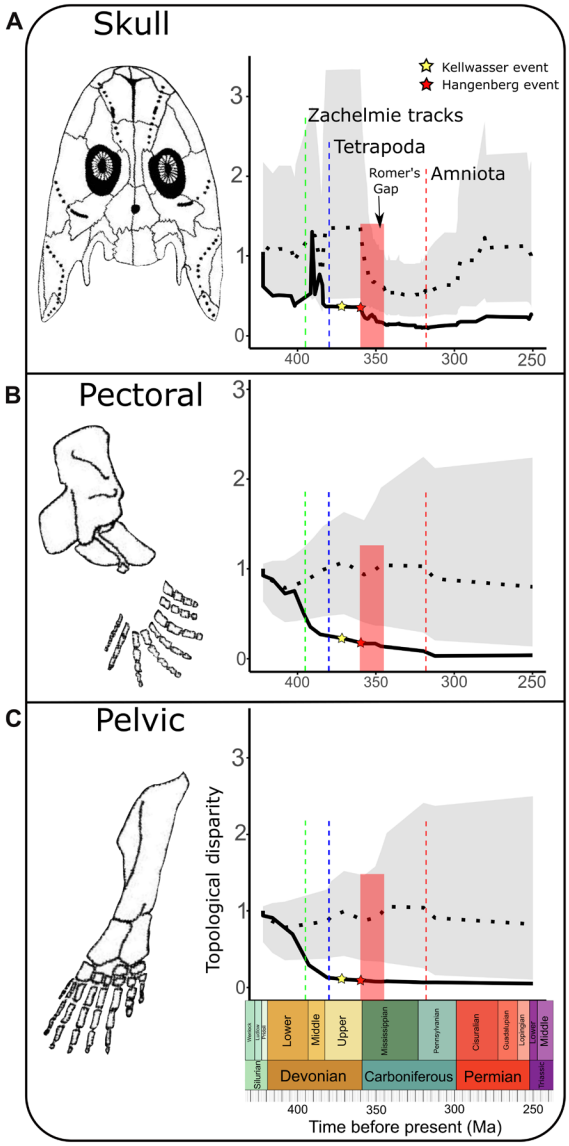

Fig. 5. Topological DTT across the origin of tetrapods. Mean relative subclade DTT (black solid line) for fish and tetrapod skull (**A**), pectoral appendages (**B**), and pelvic appendages (**C**). Also shown is the mean of disparity for 10,000 phylogenetic simulations under Brownian motion (horizontal black dotted line) and the 95% confidence intervals of those simulations (gray areas). Vertical dashed colored lines mark the estimated time of key events in tetrapod evolution; the earliest evidence of tetrapod footprints (green); and the origin of tetrapods (blue) and amniotes (red). Also marked are two major extinctions in the Devonian: the Kellwasser event (yellow star) and the Hangenberg event (red star), as well as the period at the start of the Carboniferous known as Romer's Gap (red bar); (A) uses the topology of tree A; DTT plot using tree B is found in fig. S5. Skeletal of *Acanthostega* was taken from Clack (*2*).

connectiveness in the posterior portion of the skull, where the loss of the gill cover bones enabled the acquisition of a neck that facilitated independent mobility of the head to aid with feeding in benthic settings (*45*). The need for a more mechanically resilient skull associated with a shift from suction feeding to biting could promote increased connectiveness in the anterior snout. However, this conflicts with current evidence that tetrapodomorph fish used biting to some degree (*17*) despite maintaining a distinctly fish-like skull topology, while early tetrapods like *Acanthostega* also retained suction feeding (*12*, *18*) despite showing a more densely connected skull. *Tiktaalik rosae*, a key species in the fish-tetrapod lineage, shows an intermediate condition between suction feeding and biting (*14*). More biomechanical modeling of the skull across the origin of tetrapods is needed to resolve this, but changes to ossification during development could also explain the loss of sparsely connected anterior skull bones. Ossification sequences for the dermal skull bones of tetrapodomorph fish are currently unknown; the smallest preserved *Eusthenopteron foordi* already have a fully ossified cranium (*46*), although, in *Amia calva*, the nasal and rostral bones ossify after the tooth-bearing elements and around the same time as other anterior dermal bones (*47*). Failure to ossify and bone fusion caused by developmental truncation are thought to be responsible for drastic reduction in skull bone number in batrachians (*37*), and similar process could conceivably have driven a trend toward more densely connected skulls with fewer elements in the earliest tetrapods.

Our finding of decreasing cranial bone number across the fish-tetrapod transition is coincident with other major evolutionary transitions such as the origin of mammals (*22*), turtles (*26*), squamates (*27*), and birds (*28*), yet this decrease is associated with an increase in topological complexity. We do not find evidence of increased disparity in cranial construction associated with this increased complexity. We find the opposite, suggesting that, for early tetrapods at least, decreasing bone count is not driving the evolution of morphological diversity. Following the evolution of tetrapods, topological disparity remains significantly below that expected from Brownian motion for the entirety of the Palaeozoic, suggesting that changes in disparity are actively constrained. It appears that modifications to skull topology at the origin of tetrapods laid the foundation for the topological relationships of cranial bones that persisted throughout the Palaeozoic; tetrapods arrive at a particular constructional organization of the cranium that varies little over millions of years. These topological relationships persisted even as tetrapod skull morphological diversity and ecological disparity increased in the Carboniferous and into the Permian (*48*). We hypothesize that this reduced disparity and stasis may be the result of developmental constraint (canalization) and/or due to the influence of a mechanical constraint associated with the separation of the head, neck, and shoulder. *Tiktaalik* and limbed sarcopterygians reduce the dermal components of the bony opercular region and expand the endochondral scapulocoracoid, modifications associated with increased and independent mobility of the head and neck (*3*, *14*, *49*).

That said, our results show an offset in the timing of fins/limbs and the skull in early tetrapod evolution. Evidence suggests that the pectoral and pelvic fins evolved in parallel during the fin-to-limb transition (*6*, *50*), and both appendages show coincident drops in topological disparity alongside the appearance of the first tetrapod tracks (*6*). Our study shows that cranial evolution is offset from limb evolution by an estimated 10 Ma, with decreases in cranial topological disparity occurring after the first trackway evidence. Despite an early drop in the Lower Devonian, cranial topological disparity increases between the first trackway and the first osteological evidence for tetrapods, while pectoral and pelvic appendage disparity decreases. Only later does cranial topological disparity drop below that expected due to Brownian motion evolution. This suggests that different selection pressures were driving fin/limb and cranial evolution. This may be due to the use of limbs and digits and digit-like structures

for locomoting across substrates either in aquatic or terrestrial environments, while feeding ecology remained largely unchanged. Although neck mobility in *Tiktaalik* predates the evolution of digits (*3*, *14*, *45*, *49*), the onset of protracted topological constraints in cranial anatomy coincides with the freeing of the dorsal shoulder from the body wall and independent mobility of the head, neck, and shoulder, as seen in taxa such as *Ichthyostega*, *Tulerpeton*, and crown tetrapods (*45*).

We see a second, smaller drop in skull topological disparity that coincides with the Hangenberg event at the end of the Famennian (358.9 Ma), a period of mass extinction associated with a major turnover of marine and freshwater vertebrate faunas, including the decline of many sarcopterygian groups (*50*). Tetrapods have classically been included among these groups, with tetrapod remains scarcely being found during the first 15 Ma of the Carboniferous, a period known as Romer's Gap (*51*). The loss of species diversity during the Hangenberg event appears to have affected skull topological disparity as many basal tetrapod lineages became extinct, although the drop in disparity and the extinction event are less clearly linked when using tree B (fig. S5). We do not see a recovery of topological disparity following Romer's Gap and into the Late Carboniferous; disparity remains below Devonian levels despite an increase in the number of sampled species (fig. S4) as tetrapods radiated in both terrestrial and aquatic environments.

In conclusion, we find that the reduction in bone count across the origin of tetrapods is associated with an increase in complexity of articulations and a more interconnected, less modular skull topology. However, contrary to predictions, these anatomical changes led to reduced variance in topological complexity that occurs before the first osteological evidence for tetrapods in the fossil record. Very low cranial topological variance persists through the Devonian and Carboniferous and may be the result of a developmental and/or mechanical constraints associated with the evolution of the neck and loss and fusion of anterior snout bones. These changes in cranial morphology lag behind the modifications to fin-to-limb anatomy that are commensurate with the first evidence for tetrapod tracks. This suggests that different evolutionary drivers for fin-limb and cranial evolution were at play during the evolution of tetrapods.

MATERIALS AND METHODS

Network modeling

We built unweighted, undirected network models for the skull of each taxon, in which nodes were coded for bones and links connecting nodes were coded for physical articulation or contacts between two bones. Extinct taxa were selected only if well-preserved skulls and well-supported reconstructions were available in the literature. Disarticulated materials were considered only in cases where the skull anatomy was sufficiently preserved as to allow for a complete reconstruction. Extant taxa were selected on the basis of available anatomical data and their phylogenetic position bracketing the water-land transition (fish rootward and Lissamphibia and amniotes crownward). Network models included the dermal bones of the skull roof, palate, and braincase. Dermal bones that show limited connection to the skull in some taxa (i.e., septomaxillae in early tetrapods and maxillae in some fish and Lissamphibia) were only included in the network if they showed an unequivocal sutural contact to the surrounding bones in figures or accompanying osteological descriptions; superficial dermal bones were not considered. The hyomandibular and stapes were included in taxa where these elements form structural components of the skull and are firmly attached to surrounding bones, as is found in some fish and early tetrapodomorphs. In rare cases when a single bone is formed by a mosaic of small asymmetrical elements, such as the supraorbital in *Atractosteus*, we coded them as a single node for two reasons: First, these arrays of bones show substantial variation among individuals and often between the left and right sides of a single individual; second, their absence in tetrapod taxa, and their sheer number in some cases, means their inclusion would have a disproportionate impact on the results. In cases where sutural contacts were not explicitly stated or when articular surfaces were not preserved, adjacency in reconstructions was considered sufficient justification to code a contact. All skull network models constructed for this study are available on the University of Bristol data repository, data.bris, at https://doi.org/10.5523/bris.e0ea0wn9tby12sxvckwxlcefj. Network models for pectoral and pelvic appendages of fish and early tetrapods for the comparative DTT analysis were taken from Esteve-Altava *et al.* (*23*).

Phylogenetic relationships

Two phylogenetic trees were assembled for our study taxa to test the effect of alternative phylogenetic hypotheses of tetrapod relationships, most notably the position of Lissamphibia. Tree A, based on Marjanović and Laurin (*52*), places Lissamphibia within Lepospondyli, while tree B, based on Ruta *et al.* (*53*), places them within Temnospondyli. To cover all taxa sampled in our study, the original trees were pruned of unused tips using the ape package (*54*) in R, and additional taxa were added when required using the phangorn package (*55*). The position of additional taxa in the tree was determined using phylogenetic studies published in the literature for anurans (*56*), caudates (*57*), amniotes (*58*), lepospondyls (*59*), temnospondyls (*60*), osteolepiforms (*61*), coelacanths (*62*), and major relationships between Osteichthyes (*63*). Following the work of Ruta *et al.*, we calibrated the tree branches using the "equal" method implemented in the package paleotree (*64*) for R. This method makes few assumptions about divergence times and relies exclusively on first appearance dates. Temporal ranges of taxa using first and last appearance dates were taken from the Paleobiology Database (https://paleobiodb.org/) and can be found in data S1. For extant taxa where fossil data was not available, estimated first appearance dates were taken from the literature [Jetz and Pyron (*65*) for Lissamphibia, Zheng and Wiens (*66*) for squamates, and Sugeha *et al.* (*67*) for *Latimeria*]. We constrained tree calibration by assigning minimum dates for known internal nodes based on molecular inferences and fossil dates from the literature (table S3). The completed calibrated trees can be found at the University of Bristol data repository, data.bris, at https://doi.org/10.5523/bris.e0ea0wn9tby12sxvckwxlcefj.

Analysis of topological variation

We measured eight topological variables from each network model (data S2) using the R package igraph (*68*), the details of which are shown in Fig. 1. For further mathematical details of each variable, including details of the community detection algorithm used to measure parcellation, see the Supplementary Materials. To analyze similarities in anatomical organization among skulls, we first performed a PCA of the eight topological variables, by a singular value decomposition of the centered and scaled measures, using the function prcomp in the R built-in package stats (*69*). Then, we tested for statistically significant differences in anatomical organization between fish and tetrapod skulls, as well as between each major clade, using

a phylogenetic PERMANOVA with 10,000 permutations, as implemented in the function adonis in the R package vegan (*70*). PERMANOVA uses a permutation test with pseudo-*F* ratios on the Euclidean distances of the matrix of PCA components to test the null hypothesis that the centroids and dispersion are equivalent for each group comparison. Thus, rejecting the null hypothesis means that the anatomical organization of skulls differs between the groups compared. Last, we performed a PGLS regression analysis between the number of bones (*N*) and topological variables *D*, *C*, *L*, *H*, *A*, and *P* to test the effect of bone loss on skull architecture in each clade. The analysis was performed in R using the pgls function in the package caper (*71*), estimating lambda with maximum likelihood.

Robustness of topological variables

To assess the robustness of our analyses against potential error in identifying the presence of bone articulations, we compared the eight topological variables measured for each network against a randomly generated sample of 10,000 noisy networks. Each noisy network was generated by randomly changing the links in the original network with a 0.05 probability, creating a network with 5% error from the original. We tested the null hypothesis that our measured network values were equal to the sample mean of noisy networks, which was rejected with $\alpha = 0.05$ if the observed value is in the 5% end of the distribution of simulated values. Of the 904 (8 variables × 113 networks) values tested, only 2 (0.22%) fell outside of the confidence intervals. These were heterogeneity in *Eoherpeton* and clustering in *Mandageria*. This indicates that the overwhelming majority of our measured variables would be unaffected even if 5% of bone articulations were coded erroneously in each network.

Disparity through time

Topological DTT was assessed using the mean relative subclade DTT for the two phylogenetic hypotheses. We used the covariation of topological variables from our PCAs to calculate the mean subclade disparity on the PC scores using the function dtt in the R package Geiger (*72*). The higher the disparity, the higher the variance within subclades (i.e., lower conservation) and the lower the variance between subclades. Function dtt also calculated the MDI, which quantified the overall difference in relative disparity between that shown by the DTT trend line for the time range of our fossil sample (422 to 150 Ma) and that expected under the null Brownian motion model. The statistical significance of this difference was tested using a randomization inference test with 10,000 simulations under a Brownian motion model of evolution, with the null hypothesis that the DTT trend line would fall within the 95% confidence intervals of the Brownian motion model.

Study limitations

We chose to focus on complete and well-preserved skulls to avoid uncertainty about unknown anatomies. For this reason, we did not include species with incomplete preservation. This includes the tetrapodomorph fish *Elpistostege*, which lacks a full skull reconstruction in the literature. The decrease in the number of described tetrapods from Romer's Gap is reflected in our study, and relatively few skull networks from this period are included in our dataset. Recent discoveries of Tournaisian and Visean tetrapods such as *Aytonerpeton* and *Koilops* (*73*) have suggested that Romer's Gap may not have been as sparsely populated by tetrapods as previously thought, but these species are not well-preserved enough to be included here. Consequently, there is the possibility that the structural disparity of tetrapods during the early Carboniferous is underestimated, and its decay may not be as severe as shown in our results.

SUPPLEMENTARY MATERIALS

Supplementary material for this article is available at https://science.org/doi/10.1126/sciadv.adc8875

View/request a protocol for this paper from *Bio-protocol*.

REFERENCES AND NOTES

1. J. A. Clack, The fish–tetrapod transition: New fossils and interpretations. *Evol. Educ. Outreach* **2**, 213–223 (2009).
2. J. A. Clack, *Gaining Ground: The Origin and Evolution of Tetrapods*. (Indiana Univ. Press, 2012).
3. N. H. Shubin, E. B. Daeschler, F. A. Jenkins, The pectoral fin of *Tiktaalik roseae* and the origin of the tetrapod limb. *Nature* **440**, 764–771 (2006).
4. R. Cloutier, A. M. Clement, M. S. Lee, R. Noël, I. Béchard, V. Roy, J. A. Long, Elpistostege and the origin of the vertebrate hand. *Nature* **579**, 549–554 (2020).
5. P. A. Beznosov, J. A. Clack, E. Lukševičs, M. Ruta, P. E. Ahlberg, Morphology of the earliest reconstructable tetrapod Parmastega aelidae. *Nature* **574**, 527–531 (2019).
6. B. Esteve-Altava, S. E. Pierce, J. L. Molnar, P. Johnston, R. Diogo, J. R. Hutchinson, Evolutionary parallelisms of pectoral and pelvic network-anatomy from fins to limbs. *Sci. Adv.* **5**, eaau7459 (2019).
7. B. V. Dickson, J. A. Clack, T. R. Smithson, S. E. Pierce, Functional adaptive landscapes predict terrestrial capacity at the origin of limbs. *Nature* **589**, 242–245 (2021).
8. Z. Johanson, J. M. Joss, C. A. Boisvert, R. Ericsson, M. Sutija, P. E. Ahlberg, Fish fingers: Digit homologues in sarcopterygian fish fins. *J. Exp. Zool. Part B* **308**, 757–768 (2007).
9. B. K. Hall, *Fins Into Limbs: Evolution, Development, and Transformation* (University of Chicago Press, 2008).
10. F. Langellotto, M. Fiorentino, E. De Felice, L. Caputi, V. Nittoli, J. M. Joss, P. Sordino, Expression of *meis* and *hoxa11* in dipnoan and teleost fins provides new insights into the evolution of vertebrate appendages. *EvoDevo* **9**, 11 (2018).
11. J. M. Woltering, I. Irisarri, R. Ericsson, J. M. P. Joss, P. Sordino, A. Meyer, Sarcopterygian fin ontogeny elucidates the origin of hands with digits. *Sci. Adv.* **6**, eabc3510 (2020).
12. J. M. Neenan, M. Ruta, J. A. Clack, E. J. Rayfield, Feeding biomechanics in Acanthostega and across the fish–tetrapod transition. *Proc. R. Soc. B* **281**, 20132689 (2014).
13. P. E. Ahlberg, J. A. Clack, E. Lukševičs, Rapid braincase evolution between *Panderichthys* and the earliest tetrapods. *Nature* **381**, 61–64 (1996).
14. J. B. Lemberg, E. B. Daeschler, N. H. Shubin, The feeding system of *Tiktaalik roseae*: An intermediate between suction feeding and biting. *Proc. Natl. Acad. Sci. U.S.A.* **118**, e2016421118 (2021).
15. M. J. Markey, C. R. Marshall, Terrestrial-style feeding in a very early aquatic tetrapod is supported by evidence from experimental analysis of suture morphology. *Proc. Natl. Acad. Sci. U.S.A.* **104**, 7134–7138 (2007).
16. T. R. Simões, S. E. Pierce, Sustained high rates of morphological evolution during the rise of tetrapods. *Nat. Ecol. Evol.* **5**, 1403–1414 (2021).
17. L. B. Porro, E. J. Rayfield, J. A. Clack, Computed tomography, anatomical description and three-dimensional reconstruction of the lower jaw of *Eusthenopteron foordi* Whiteaves, 1881 from the Upper Devonian of Canada. *Palaeontology* **58**, 1031–1047 (2015).
18. L. B. Porro, E. J. Rayfield, J. A. Clack, Descriptive anatomy and three-dimensional reconstruction of the skull of the early tetrapod Acanthostega gunnari Jarvik, 1952. *PLOS ONE* **10**, e0118882 (2015).
19. E. Heiss, P. Aerts, S. Van Wassenbergh, Aquatic–terrestrial transitions of feeding systems in vertebrates: A mechanical perspective. *J. Exp. Biol.* **221**, jeb154427 (2018).
20. S. Van Wassenbergh, in *Feeding in Vertebrates* (Springer International Publishing, 2019), pp. 139–158.
21. P. S. Anderson, M. Friedman, M. Ruta, Late to the table: Diversification of tetrapod mandibular biomechanics lagged behind the evolution of terrestriality. *Integr. Comp. Biol.* **53**, 197–208 (2013).
22. C. A. Sidor, Simplification as a trend in synapsid cranial evolution. *Evolution* **55**, 1419–1442 (2001).
23. B. Esteve-Altava, J. Marugán-Lobón, H. Botella, D. Rasskin-Gutman, Structural constraints in the evolution of the tetrapod skull complexity: Williston's law revisited using network models. *Evol. Biol.* **40**, 209–219 (2013).
24. B. Esteve-Altava, J. Marugán-Lobón, H. Botella, D. Rasskin-Gutman, Random loss and selective fusion of bones originate morphological complexity trends in tetrapod skull networks. *Evol. Biol.* **41**, 52–61 (2014).
25. C. A. Sidor, Evolutionary trends and the origin of the mammalian lower jaw. *Paleobiology* **29**, 605–640 (2003).

26. E. S. Gaffney, Comparative cranial morphology of Recent and fossil turtles. *Bull. Am. Mus. Nat. Hist.* **164**, 65–375 (1979).
27. A. Herrel, V. Schaerlaeken, J. J. Meyers, K. A. Metzger, C. F. Ross, The evolution of cranial design and performance in squamates: Consequences of skull-bone reduction on feeding behavior. *Integr. Comp. Biol.* **47**, 107–117 (2007).
28. O. Plateau, C. Foth, Birds have peramorphic skulls, too: Anatomical network analyses reveal oppositional heterochronies in avian skull evolution. *Commun. Biol.* **3**, 195 (2020).
29. W. K. Gregory, 'Williston's law' relating to the evolution of skull bones in the vertebrates. *Am. J. Phys. Anthropol.* **20**, 123–152 (1935).
30. M. Moazen, N. Curtis, P. O'Higgins, S. E. Evans, M. J. Fagan, Biomechanical assessment of evolutionary changes in the lepidosaurian skull. *Proc. Natl. Acad. Sci. U.S.A.* **106**, 8273–8277 (2009).
31. B. Esteve-Altava, J. Marugan-Lobon, H. Botella, D. Rasskin-Gutman, Network models in anatomical systems. *J. Anthropol. Sci.* **89**, 175–184 (2011).
32. J. D. Pardo, M. Szostakiwskyj, P. E. Ahlberg, J. S. Anderson, Hidden morphological diversity among early tetrapods. *Nature* **546**, 642–645 (2017).
33. J. R. Rawson, L. B. Porro, E. Martin-Silverstone, E. J. Rayfield, Osteology and digital reconstruction of the skull of the early tetrapod *Whatcheeria deltae*. *J. Vertebr. Paleontol.* **41**, e1927749 (2021).
34. G. Niedźwiedzki, P. Szrek, K. Narkiewicz, M. Narkiewicz, P. E. Ahlberg, Tetrapod trackways from the early Middle Devonian period of Poland. *Nature* **463**, 43–48 (2010).
35. P. E. Ahlberg, Elginerpeton pancheni and the earliest tetrapod clade. *Nature* **373**, 420–425 (1995).
36. K. Pawley, A. Warren, The appendicular skeleton of *Eryops megacephalus* COPE, 1877 (Temnospondyli: Eryopoidea) from the lower permian of North America. *J. Paleo.* **80**, 561–580 (2006).
37. R. R. Schoch, Amphibian skull evolution: The developmental and functional context of simplification, bone loss and heterotopy. *J. Exp. Zool. Part B* **322**, 619–630 (2014).
38. F. O. Da Silva, A.-C. Fabre, Y. Savriama, J. Ollonen, K. Mahlow, A. Herrel, J. Müller, N. Di-Poï, The ecological origins of snakes as revealed by skull evolution. *Nat. Commun.* **9**, 376 (2018).
39. R. R. Schoch, R. Werneburg, S. Voigt, A Triassic stem-salamander from Kyrgyzstan and the origin of salamanders. *Proc. Natl. Acad. Sci. U.S.A.* **117**, 11584–11588 (2020).
40. M. W. Caldwell, R. L. Nydam, A. Palci, S. Apesteguía, The oldest known snakes from the Middle Jurassic-Lower Cretaceous provide insights on snake evolution. *Nat. Commun.* **6**, 5996 (2015).
41. E. Vorobyeva, H. -P. Schultze, Relationship to Tetrapods, in *Origins of the Higher Groups of Tetrapods: Controversy and Consensus* (Cornell Univ. Press, 1991).
42. P. E. Ahlberg, J. A. Clack, E. Lukševičs, H. Blom, I. Zupiņš, Ventastega curonica and the origin of tetrapod morphology. *Nature* **453**, 1199–1204 (2008).
43. M. Coates, J. A. Clack, Fish-like gills and breathing in the earliest known tetrapod. *Nature* **352**, 234–236 (1991).
44. A. Kemp, Skull structure in post-Paleozoic lungfish. *J. Vertebr. Paleontol.* **18**, 43–63 (1998).
45. N. Shubin, E. B. Daeschler, F. A. Jenkins, in *Great Transformations in Vertebrate Evolution* (University of Chicago Press, 2021), pp. 63–76.
46. S. Cote, R. Carroll, R. Cloutier, L. Bar-Sagi, Vertebral development in the Devonian sarcopterygian fish *Eusthenopteron foordi* and the polarity of vertebral evolution in non-amniote tetrapods. *J. Vertebr. Paleontol.* **22**, 487–502 (2002).
47. L. Grande, W. E. Bemis, A comprehensive phylogenetic study of amiid fishes (Amiidae) based on comparative skeletal anatomy. An empirical search for interconnected patterns of natural history. *J. Vertebr. Paleontol.* **18**, 1–696 (1998).
48. J. A. Clack, M. Ruta, A. R. Milner, J. E. Marshall, T. R. Smithson, K. Z. Smithson, *Acherontiscus caledoniae*: The earliest heterodont and durophagous tetrapod. *R. Soc. Open Sci.* **6**, 182087 (2019).
49. N. H. Shubin, E. B. Daeschler, F. A. Jenkins, Pelvic girdle and fin of *Tiktaalik roseae*. *Proc. Natl. Acad. Sci. U.S.A.* **111**, 893–899 (2014).
50. L. C. Sallan, M. I. Coates, End-Devonian extinction and a bottleneck in the early evolution of modern jawed vertebrates. *Proc. Natl. Acad. Sci. U.S.A.* **107**, 10131–10135 (2010).
51. P. Ward, C. Labandeira, M. Laurin, R. A. Berner, Confirmation of Romer's Gap as a low oxygen interval constraining the timing of initial arthropod and vertebrate terrestrialization. *Proc. Natl. Acad. Sci. U.S.A.* **103**, 16818–16822 (2006).
52. D. Marjanović, M. Laurin, Phylogeny of Paleozoic limbed vertebrates reassessed through revision and expansion of the largest published relevant data matrix. *PeerJ* **6**, e5565 (2019).
53. M. Ruta, J. Krieger, K. D. Angielczyk, M. A. Wills, The evolution of the tetrapod humerus: Morphometrics, disparity, and evolutionary rates. *Earth Environ. Sci. Trans. R. Soc. Edinb.* **109**, 351–369 (2018).
54. E. Paradis, J. Claude, K. Strimmer, APE: Analyses of phylogenetics and evolution in R language. *Bioinformatics* **20**, 289–290 (2004).
55. K. P. Schliep, phangorn: Phylogenetic analysis in R. *Bioinformatics* **27**, 592–593 (2011).
56. Y. -J. Feng, D. C. Blackburn, D. Liang, D. M. Hillis, D. B. Wake, D. C. Cannatella, P. Zhang, Phylogenomics reveals rapid, simultaneous diversification of three major clades of Gondwanan frogs at the Cretaceous–Paleogene boundary. *Proc. Natl. Acad. Sci. U.S.A.* **114**, E5864–E5870 (2017).
57. A. -C. Fabre, C. Bardua, M. Bon, J. Clavel, R. N. Felice, J. W. Streicher, J. Bonnel, E. L. Stanley, D. C. Blackburn, A. Goswami, Metamorphosis shapes cranial diversity and rate of evolution in salamanders. *Nat. Ecol. Evol.* **4**, 1129–1140 (2020).
58. D. P. Ford, R. B. Benson, The phylogeny of early amniotes and the affinities of Parareptilia and Varanopidae. *Nat. Ecol. Evol.* **4**, 57–65 (2020).
59. H. C. Maddin, F. A. Jenkins Jr., J. S. Anderson, The braincase of *Eocaecilia micropodia* (Lissamphibia, Gymnophiona) and the origin of caecilians. *PLOS ONE* **7**, e50743 (2012).
60. R. R. Schoch, The evolution of major temnospondyl clades: An inclusive phylogenetic analysis. *J. Syst. Palaeontol.* **11**, 673–705 (2013).
61. P. E. Ahlberg, Z. Johanson, Osteolepiforms and the ancestry of tetrapods. *Nature* **395**, 792–794 (1998).
62. P. Forey, *History of the Coelacanth Fishes* (Chapman & Hall, 1998).
63. R. Betancur-R, E. O. Wiley, G. Arratia, A. Acero, N. Bailly, M. Miya, G. Lecointre, G. Ortí, Phylogenetic classification of bony fishes. *BMC Evol. Biol.* **17**, 162 (2017).
64. D. W. Bapst, paleotree: An R package for paleontological and phylogenetic analyses of evolution. *Methods Ecol. Evol.* **3**, 803–807 (2012).
65. W. Jetz, R. A. Pyron, The interplay of past diversification and evolutionary isolation with present imperilment across the amphibian tree of life. *Nat. Ecol. Evol.* **2**, 850–858 (2018).
66. Y. Zheng, J. J. Wiens, Combining phylogenomic and supermatrix approaches, and a time-calibrated phylogeny for squamate reptiles (lizards and snakes) based on 52 genes and 4162 species. *Mol. Phylogenet. Evol.* **94**, 537–547 (2016).
67. H. Kadarusman, Y. Sugeha, L. Pouyaud, R. Hocdé, I. B. Hismayasari, E. Gunaisah, S. B. Widiarto, G. Arafat, F. Widyasari, D. Mouillot, E. Paradis, A thirteen-million-year divergence between two lineages of Indonesian coelacanths. *Sci. Rep.* **10**, 192 (2020).
68. R Core Team, R: A Language and Environment for Statistical Computing (R Foundation for Statistical Computing, 2013); www.r-project.org.
69. G. Csardi, T. Nepusz, The igraph software package for complex network research. *Int. j. complex syst* **1695**, 1–9 (2006).
70. P. Dixon, VEGAN, a package of R functions for community ecology. *J. Veg. Sci.* **14**, 927–930 (2003).
71. D. Orme, R. Freckleton, G. Thomas, T. Petzoldt, S. Fritz, The caper package: Comparative analysis of phylogenetics and evolution in R. *R package version* **5**, 1–36 (2013).
72. L. J. Harmon, J. T. Weir, C. D. Brock, R. E. Glor, W. Challenger, GEIGER: Investigating evolutionary radiations. *Bioinformatics* **24**, 129–131 (2008).
73. J. A. Clack, C. E. Bennett, D. K. Carpenter, S. J. Davies, N. C. Fraser, T. I. Kearsey, J. E. A. Marshall, D. Millward, B. K. A. Otoo, E. J. Reeves, A. J. Ross, M. Ruta, K. Z. Smithson, T. R. Smithson, S. A. Walsh, Phylogenetic and environmental context of a Tournaisian tetrapod fauna. *Nat. Ecol. Evol.* **1**, 0002 (2016).
74. E. Jarvik, "The evolutionary importance of Eusthenopteron foordi (Osteolepiformes)", in *Devonian Fishes and Plants of Miguasha, Quebec, Canada* (Verlag Dr. Friedrich Pfeil, 1996), pp. 7–11.
75. R. L. Carroll, R. Holmes, The skull and jaw musculature as guides to the ancestry of salamanders. *Zool. J. Linn. Soc.* **68**, 1–40 (1980).
76. M. Delfino, D. A. Iurino, B. Mercurio, P. Piras, L. Rook, R. Sardella, Old African fossils provide new evidence for the origin of the American crocodiles. *Sci. Rep.* **10**, 11127 (2020).
77. M. E. Newman, M. Girvan, Finding and evaluating community structure in networks. *Phys. Rev. E* **69**, 026113 (2004).
78. Y. Benjamini, Y. Hochberg, Controlling the false discovery rate: A practical and powerful approach to multiple testing. *J. R. Stat. Soc. Ser. B Methodol.* **57**, 289–300 (1995).
79. M. Zhu, W. Zhao, L. Jia, J. Lu, T. Qiao, Q. Qu, The oldest articulated osteichthyan reveals mosaic gnathostome characters. *Nature* **458**, 469–474 (2009).
80. B. Swartz, A marine stem-tetrapod from the Devonian of western North America. *PLOS ONE* **7**, e33683 (2012).
81. S. B. Hedges, S. Kumar, *The Timetree of Life* (Oxford Univ. Press, 2009).
82. M. E. Jones, C. L. Anderson, C. A. Hipsley, J. Müller, S. E. Evans, R. R. Schoch, Integration of molecules and new fossils supports a Triassic origin for Lepidosauria (lizards, snakes, and tuatara). *BMC Evol. Biol.* **13**, 208 (2013).
83. M. J. Benton, P. C. J. Donoghue, R. J. Asher, M. Friedman, T. J. Near, J. Vinther, Constraints on the timescale of animal evolutionary history. *Palaeontol. Electron.* **18**, 1–106 (2015).

Acknowledgments: We thank J. Bolt (FMNH), S. Chapman (NHM), J. Clack (UMZC), G. Cuny (MGUH), S. Desbiens (MNHN), E. Lombard (University of Chicago), M. Lowe (UMZC), E. Luksevics (University of Latvia), W. Simpson (FMNH), A. Stroup (FMNH), and S. Wild (BGS) for loan of fossil specimens and A. Herrel (MNHN), J. Yves-Sire (MNHN), and M. Westneat (University of Chicago) for providing extant specimens. CT scans of specimens were provided by P. Ahlberg (University of Uppsala), M. Arsenault (Miguasha National Park, Québec, Canada), E. Herbst (Universität Zürich), J. Hutchinson (RVC), and T. Rowe (University of Texas at Austin).

Original CT scanning was carried out by M. Colbert and R. Ketcham (UTCT, University of Texas at Austin); T. Davies, B. Moon, and L. Martin-Silverstone (Bristol); A. Neander (University of Chicago); K. Smithson and L.B.P. (Cambridge); A. Ramsey (Tring); and D. Sykes (NHM). We also thank M. Ruta (University of Lincoln) for advice on early tetrapod phylogenetics and A. Sánchez-Eróstegui and J.-L. Garnier (Thermo Fisher Scientific) for assistance with Avizo. **Funding:** This work was supported by NERC standard grant NE/P013090/1 ("Skull evolution and the terrestrialization and radiation of tetrapods") (E.J.R. and L.B.P.); Marie Curie International Incoming Research Fellowship 303161 (Tetrapods Rising) (L.B.P.); "la Caixa" Banking Foundation Postdoctoral Junior Leader Fellowship Programme, LCF/BQ/LI18/11630002 (B.E.-A.); and Palaeontological Association Undergraduate Research Bursary, PA-UB202006 (J.R.G.R.). **Author contributions:** Conceptualization: B.E.-A., L.B.P., H.D., and E.J.R. Methodology: J.R.G.R., B.E.-A., L.B.P., H.D., and E.J.R. Data collection and analysis: J.R.G.R. and B.E.-A. Data interpretation and discussion: J.R.G.R., B.E.-A., L.B.P., H.D., and E.J.R. Writing—main draft: J.R.G.R. and E.J.R. Writing—review and editing: J.R.G.R., B.E.-A., L.B.P, H.D., and E.J.R. **Competing interests:** The authors declare that they have no competing interests. **Data and materials availability:** The data and code that support the findings of this study are available from the University of Bristol data repository, data.bris, at https://doi.org/10.5523/bris.e0ea0wn9tby12sxvckwxlcefj. All data needed to evaluate the conclusions in the paper are present in the paper and/or the Supplementary Materials.

Submitted 6 May 2022
Accepted 26 July 2022
Published 9 September 2022
10.1126/sciadv.adc8875